Biochemistry and Biophysics Reports 11 (2017) 58–63

Contents lists available at ScienceDirect

Biochemistry and Biophysics Reports

journal homepage: www.elsevier.com/locate/bbrep

Vesicle fusion with bilayer lipid membrane controlled by electrostatic interaction

Azusa Oshima*, Koji Sumitomo[1]

NTT Basic Research Laboratories, NTT Corporation, 3-1 Morinosato Wakamiya, Atsugi, Kanagawa 243-0198, Japan

A B S T R A C T

The fusion of proteoliposomes is a promising approach for incorporating membrane proteins in artificial lipid membranes. In this study, we employed an electrostatic interaction between vesicles and supported bilayer lipid membranes (s-BLMs) to control the fusion process. We combined large unilamellar vesicles (LUVs) containing anionic lipids, which we used instead of proteoliposomes, and s-BLMs containing cationic lipids to control electrostatic interaction. Anionic LUVs were never adsorbed or ruptured on the SiO_2 substrate with a slight negative charge, and selectively fused with cationic s-BLMs. The LUVs can be fused effectively to the target position. Furthermore, as the vesicle fusion proceeds and some of the positive charges are neutralized, the attractive interaction weakens and finally the vesicle fusion saturates. In other words, we can control the number of LUVs fused with s-BLMs by controlling the concentration of the cationic lipids in the s-BLMs. The fluidity of the s-BLMs after vesicle fusion was confirmed to be sufficiently high. This indicates that the LUVs attached to the s-BLMs were almost completely fused, and there were few intermediate state vesicles in the fusion process. We could control the position and amount of vesicle fusion with the s-BLMs by employing an electrostatic interaction.

1. Introduction

Artificial bilayer lipid membranes (BLMs) are simple models with which to understand the functional and structural complexity of cellular systems under chemically controlled conditions [1,2]. The basic properties of a lipid membrane (fluidity, continuity, and defects [3]) and related phenomena (vesicle fusion [4] and phase separation [5]), which have been actively studied by using artificial BLMs, constitute indispensable knowledge as regards understanding biological phenomena. In addition, systems combining artificial BLMs and membrane proteins extracted from biological cells are useful for understanding the function of membrane proteins [6]. Membrane proteins, which contribute to signal transduction and material transport in biological cells, do not function without a lipid membrane. When the proteins of interest are purified and reconstituted into artificial BLMs, it is possible to undertake their functional analysis while completely excluding the contributions of untargeted proteins [6]. Assay systems that combine membrane proteins and artificial BLMs have also been proposed and extensively studied. The combination of semiconductor micro- or nanofabrication techniques and artificial BLMs with membrane proteins is a promising approach as regards device application [7–10]. We have reported that Ca^{2+} ion transport through an α-hemolysin channel could be analyzed by observing the fluorescence of microwells sealed by BLMs on a Si substrate [9]. The insertion of toxin-type ion channels such as α-hemolysin into BLMs occurs spontaneously when they are added to the solution. However, when trying to extend this system to receptor proteins (e.g. ionotropic glutamate receptors [11]), insertion into the BLMs is not so simple [12]. One promising approach is the vesicle fusion of proteoliposomes, which are vesicles containing membrane proteins, into the BLMs [6]. To promote vesicle fusion, additional factors such as osmotic pressure [13], SNARE protein [14,15], DNA [16], and centrifugal force [17] have been proposed. Electrostatic interaction is also widely used to control and promote vesicle fusion [4]. Electrostatic attraction between cells and cationic vesicles has also been commonly used for transfection [18]. In this study, we investigated vesicle fusion under electrostatic attractive interaction with supported bilayer lipid membranes (s-BLMs) on a SiO_2 substrate. Since the surface of a SiO_2 substrate is negatively charged in most of the pH range [19], we adopted a combination of cationic s-BLMs and anionic vesicles, as shown in Fig. 1. We tried to control the position and the amount of vesicle fusion. The knowledge obtained in this study will be extended to the fusion of proteoliposomes and contribute to the arrangement of

* Corresponding author.
E-mail address: oshima.azusa@lab.ntt.co.jp (A. Oshima).
[1] Present address: University of Hyogo, 2167 Shosha, Himeji, Hyogo 671-2280, Japan.

http://dx.doi.org/10.1016/j.bbrep.2017.06.003
Received 17 March 2017; Received in revised form 16 May 2017; Accepted 16 June 2017
Available online 19 June 2017

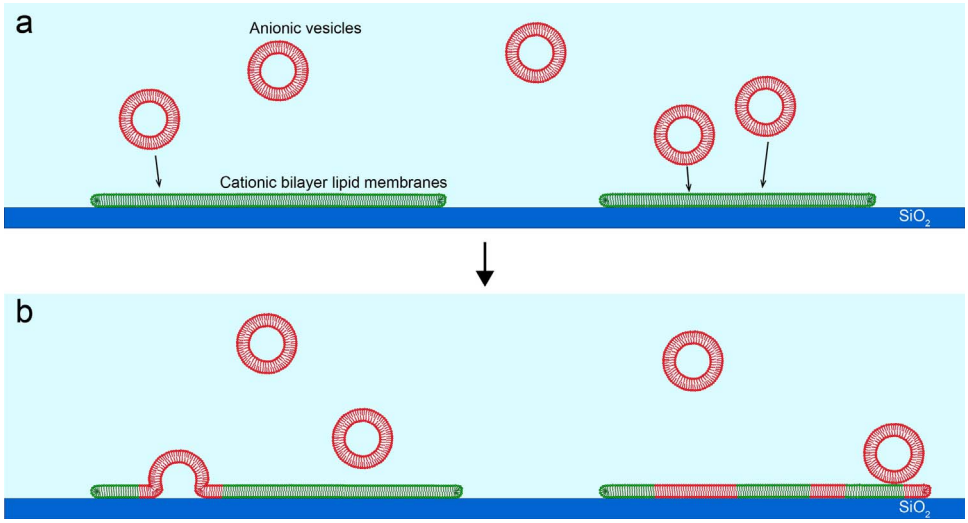

Fig. 1. Schematic images of vesicle fusion by electrostatic interaction. (a) Cationic s-BLMs (shown in green) were placed on a negatively charged SiO_2 substrate. (b) After adding anionic vesicles (shown in red), vesicles preferentially attached to and fused with the cationic s-BLMs.

membrane proteins for device applications.

2. Materials and methods

2.1. Materials

1,2-diphytanoyl-*sn*-glycero-3-phosphocholine (DPhPC), 1,2-dioleoyl-*sn*-glycero-3-phosphocholine (DOPC), 1,2-dioleoyl-*sn*-glycero-3-ethylphosphocholine (EDOPC), 1,2-dioleoyl-*sn*-glycero-3-phospho-L-serine (sodium salt) (DOPS), 2-dioleoyl-*sn*-glycero-3-phosphoethanolamine-*N*-(7-nitro-2-1,3-benzoxadiazol-4-yl) (ammonium salt) (NBD-DOPE), and 1,2-dipalmitoyl-*sn*-glycero-3-phosphoethanolamine-*N*-(lissamine rhodamine B sulfonyl) (ammonium salt) (Rhod-DPPE) were purchased from Avanti Polar Lipids (Alabaster AL). Cholesterol (Chol) was purchased from Avanti Polar Lipids or obtained from Wako Pure Chemicals (Osaka, Japan) and recrystallized three times from methanol.

2.2. GUV preparation

The s-BLMs were prepared by rupturing giant unilamellar vesicles (GUVs). Cationic GUVs were prepared by the electroformation method [20] from EDOPC, DPhPC and cholesterol (x:80-x:20). EDOPC is a biocompatible synthetic lipid with one positive net charge per molecule. The concentration (x) of the cationic lipids in the cationic GUVs was in the 5–20% range. These GUVs contained 0.5 mol% NBD-DOPE for labeling the lipid membranes. As a control experiment, we also prepared neutral GUVs that contained no EDOPC (x = 0). The typical conditions for the electroformation of GUVs in this study were as follows. A chloroform solution of a lipid mixture with a final concentration of 2.5 mM was spread evenly on an indium tin oxide (ITO)-coated glass slide. The slide was dried in a vacuum for 2 h, and then a chamber was constructed from a lipid-coated slide and an uncoated slide coupled with 1-mm-thick silicone rubber. The chamber was filled with sucrose solution (200 mM). The GUVs were grown by supplying an AC voltage of 1 V at 10 Hz for 2 h at 60 °C. It is somewhat difficult to form GUVs by the electroformation method when they are mixed with cationic lipids. The average diameter of a cationic GUV is smaller than that of a neutral GUV. However, under the experimental condition we used for electroformation, we were able to obtain GUVs with diameters exceeding 10 μm. This is large enough for our purpose in this study and for future applications.

2.3. LUV preparation

Anionic large unilamellar vesicles (LUVs) were prepared from DOPS and DOPC (10:90). Rhod-DPPE at 0.5 mol% was used for labeling the lipid membrane. A chloroform solution of anionic lipid was dried in a glass vial and suspended in sucrose solution (200 mM) at a lipid concentration of 5 mM. The lipid suspension, which consisted of multi-lamellar vesicles, was frozen and thawed five times. In this step, the multi-lamellar vesicles became unilamellar vesicles [21]. To obtain uniformly sized vesicles the unilamellar vesicles were extruded with a mini-extruder (Avanti Polar Lipids) using a Nuclepore polycarbonate membrane with a pore size of 100 nm (Whatman, GE Healthcare UK Ltd.).

2.4. Formation of s-BLMs

Substrates consisting of a Si(001) wafer were covered with a thermal silicon dioxide layer (120 nm). The substrates were chemically treated with piranha solution (H_2SO_4: H_2O_2 = 2: 1), followed by NH_4F for 3 min, and then piranha solution again. To obtain cationic s-BLMs, several microliters of dispersed cationic GUVs were added to glucose solution (200 mM) placed on a substrate, and the GUVs sank to the substrate surface. After incubation for a few minutes, the GUVs ruptured on the substrate as the result of an attractive electrostatic interaction. The excess GUVs were rinsed off with glucose solution (200 mM), and the sample was observed with a confocal laser scanning microscope FV1200-BX61 (Olympus) under a ×10 or ×40 objective lens. We used laser light sources emitting at 473 and 559 nm for excitation, and 490–540 and 575–675 nm band-pass filters to detect the fluorescence from NBD and rhodamine, respectively.

2.5. Observation of vesicle fusion

The SiO_2 substrate was placed on a microscope slide, and covered with a chamber consisting of silicone rubber and a cover slip. The chamber contained about 300 μL of glucose solution. After confirming the formation of s-BLMs, 1 μL of anionic LUV suspension, which was diluted 50 times to facilitate LUV diffusion, was added to the chamber and fusion with s-BLMs was observed. The evaporation of the solution during the 30–60 min observation can be negligible because there are few openings in the chamber. The samples were observed from the top by using an upright microscope system.

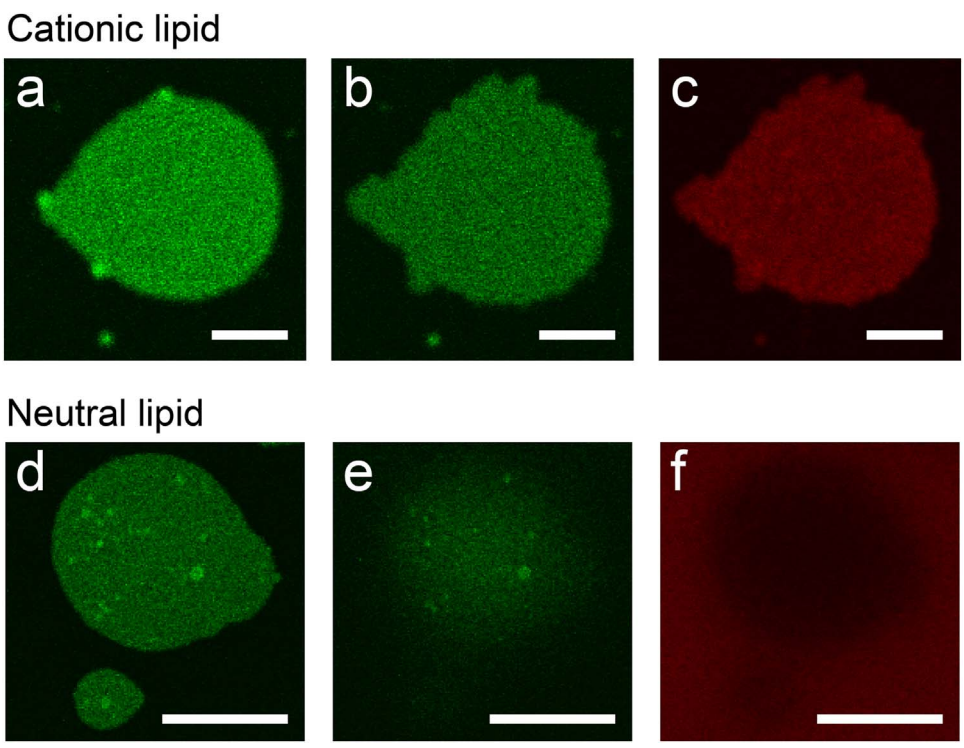

Fig. 2. Typical fluorescence microscope images of vesicle fusion. (a) Cationic s-BLMs before adding the anionic LUVs, (b)·(c) after vesicle fusion by electrostatic interaction in glucose solution (200 mM), (b) the area of s-BLMs were increased after 30 min (473 nm excitation), (c) Rhod-DPPE intensity observed at the cationic s-BLMs (559 nm excitation). (a)–(c) Scale bar: 10 μm. (d) Neutral s-BLMs before adding the anionic LUVs, (e)·(f) after vesicle fusion in glucose solution (200 mM) containing $CaCl_2{\cdot}2H_2O$ (5 mM). (e) The shape of the neutral s-BLMs was not maintained (473 nm excitation), (f) Rhod-DPPE intensity was observed at the SiO_2 substrate (559 nm excitation). (d)–(f) Scale bar: 50 μm.

3. Results and discussion

3.1. Fusion of anionic LUVs with s-BLM

Fig. 2(a) shows a fluorescence image of a patch of cationic s-BLM on the substrates (the EDOPC concentration was 10 mol%). Then, we added a solution of anionic LUVs to a chamber containing the substrate. After 30 min, the patch became slightly larger because vesicle fusion with the anionic LUVs occurred, as shown in Fig. 2(b). An increase in patch size was observed for several independent patches (n = 45) during vesicle fusion for 30–60 min, and the rate of increase $\Delta S/S$, where S is the patch area after vesicle fusion, was estimated to be 18.3 ± 8.3%. The clear observation of rhodamine fluorescence at the cationic s-BLM patch also indicates vesicle fusion (Fig. 2(c)). The rhodamine fluorescence was limited at the patch, and no fluorescence was observed on the substrate. Under this condition, since the surface of the SiO_2 substrate was slightly negatively charged, neither rupture nor adsorption was caused by the electrostatic repulsion with the anionic LUVs. Vesicle fusion occurred selectively only on the cationic s-BLM patch. Fig. 2(d)–(f) show results obtained on neutral s-BLMs for comparison. The neutral s-BLMs were formed by rupturing neutral GUVs in glucose solution (200 mM) containing $CaCl_2{\cdot}2H_2O$ (5 mM) and observed in the same solution. Even if the GUVs are neutral, their surfaces are slightly negatively charged due to the polarization of the phosphate groups in phosphatidylcholine in a solution with a pH of around 7. Therefore, vesicle fusion and rupture are suppressed by the electrostatic repulsion between the lipids and the SiO_2 substrate. Neutral s-BLMs could be formed by adding cations to the solution. Monovalent ions such as Na^+ are also effective, but divalent ions such as Ca^{2+} are more effective. It is likely that this is due to the ability of the divalent ions to "bridge" negatively charged entities such as the phosphate groups in DOPC and negative charges on the SiO_2 surface [22,23]. Fig. 2(d) shows an initial s-BLM, and Fig. 2(e) and (f) show s-BLMs after the fusion of the anionic LUVs. The rhodamine fluorescence was observed on the SiO_2 substrate after 3 min incubation, and this means that the anionic LUVs were adsorbed, ruptured, and/or fused on the substrate as well as on the s-BLM patch, as shown in Fig. 2(f). The NBD fluorescence also spread across the substrate, and did not maintain the shape of the original patch (Fig. 2(e)). After 30 min, the shape of the patch caused by the vesicle fusion process had completely disappeared. This indicates that s-BLMs were formed over the entire substrate and that there was lateral diffusion of the NBD-DOPE. With the neutral s-BLM, cations were required in the solution for s-BLM formation and for vesicle fusion to cancel the electrostatic repulsion. Therefore, it is impossible to control the fusion site. Controlling electrostatic interactions with the cationic s-BLMs is a promising method for controlling the location of vesicle fusion.

3.2. LUV fusion dependence on cationic lipid concentration

We observed the time-lapse fluorescence intensity for the vesicle fusion of different concentrations of cationic lipids to control the quantity of LUVs fused to the s-BLM patch. Fig. 3 shows a plot of the average fluorescence intensity of rhodamine at s-BLMs as a function of elapsed time. The intensity increases with elapsed time, and this indicates the progress of vesicle fusion with the s-BLMs. The fluorescence intensity could be converted to the rhodamine concentration with a calibration curve, which was obtained from fluorescent images of s-BLMs with concentration controlled rhodamine in the 0.01–0.1 mol% range. The fluorescent images for calibration were obtained with exactly the same parameters as the time lapse images. (The calibration curve is not shown here.) The amount of fusion R defined as the fraction of lipids from the fused anionic LUVs in the s-BLM patch could be estimated from the fluorescence intensity, and is shown on the right axis in Fig. 3. At the initial stage of vesicle fusion, the fluorescence intensity increased linearly. However, the rate of increase gradually slowed, and finally the intensity saturated. With a 5% concentration of cationic lipids in the s-BLMs, the time during which the intensity increased was short, and the intensity change was no longer observed after 500 s. This indicates that vesicle fusion no longer occurred. The fusion of the anionic LUVs neutralized some of the positive charges in the s-BLMs and weakened the electrostatic attractive interaction between the LUVs and the s-BLMs. Since the attractive force was no longer sufficient to induce vesicle fusion, the fluorescent intensity change became saturated. With higher cationic lipid concentrations in the s-BLMs, although the time during which the intensity increased became longer, the rate of increase

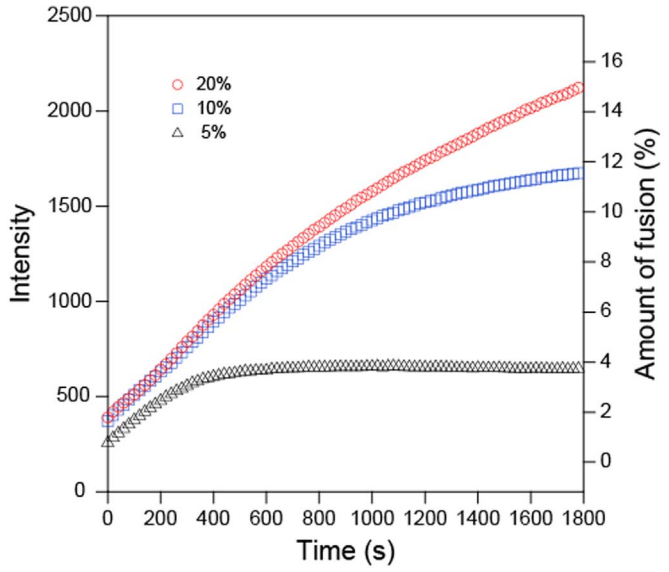

Fig. 3. The time lapse of the fluorescence intensity depended on the cationic lipid concentration. Each slope was an average of the measurements of the Rhod-DPPE intensity whose EDOPC concentrations were 5% (△black, n = 25), 10% (□blue, n = 40), and 20% (○red, n = 50).

eventually became slow and saturated. In the initial stage of vesicle fusion, LUVs that have reached the s-BLMs can fuse at a constant rate, and this is independent of the cationic lipid concentration in the s-BLMs, because the electrostatic attractive interaction is sufficiently high for vesicle fusion. However, as the vesicle fusion proceeds and some of the positive charges are neutralized, the attractive interaction becomes weaker and finally vesicle fusion is saturated.

With 5%-EDOPC in the s-BLMs, the amount of fusion for saturation was estimated to be $R = 4\%$, as shown in Fig. 3. Since the ratio of the anionic lipid (DOPS) in LUVs is 1/10, the fraction of the anionic lipid in the s-BLMs after saturation of fusion is only around 0.4%. This value is much smaller than the fraction of the cationic lipid in s-BLMs, which was estimated to be $5 \times (1 - R) = 4.8\%$. It is indicated that a considerable amount of excess cationic lipid is needed in the s-BLMs to induce vesicle fusion. This suggests that a large part of the positive charge in the s-BLMs is used to attract the negative surface charge of the SiO_2 substrate and keep the supporting membrane stably. With 10% EDOPC, the amount of fusion 1800 s after the start of vesicle fusion was estimated to be $R = 12\%$. Furthermore, it does not saturate at 1800s, but vesicle fusion continues. This value is somewhat larger than the estimated area increase $\Delta S/S = 18.3 \pm 8.3\%$, but it does not conflict if the vesicle fusion continues to occur after 1800s. When we consider the error in the area measurement, it can be regarded as consistent. When we double the cationic lipids in the s-BLMs, the amount of anionic vesicle fusion after saturation is much greater than double. This is because the proportion contributing to the interaction with the SiO_2 substrate is large while the concentration of the cationic lipid in the s-BLMs is low. When the concentration of the cationic lipid in the s-BLMs is increased above that needed to hold the supported membrane, it helps to induce vesicle fusion. Saturated fluorescent intensity, i.e. the amount of vesicle fusion, is determined by the excess positive charge in the s-BLMs. This suggests that the amount of fusion after saturation can be controlled by the initial concentration of the cationic lipid in the s-BLMs.

3.3. Fluorescence recovery after photobleaching

Next, we examined the state of the s-BLMs after vesicle fusion by employing fluorescence recovery after photobleaching (FRAP). FRAP has been commonly used to evaluate the fluidity of s-BLMs and to determine their diffusion coefficient [3]. The FRAP measurement of rhodamine, which was transferred from LUVs to s-BLMs by vesicle fusion, also enables us to evaluate the progress of vesicle fusion. Fig. 4(a)–(e) show fluorescence images of the FRAP process of the cationic s-BLMs (with an EDOPC concentration of 10 mol%) after adding the anionic

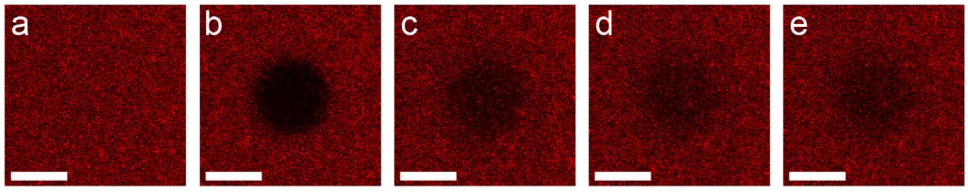

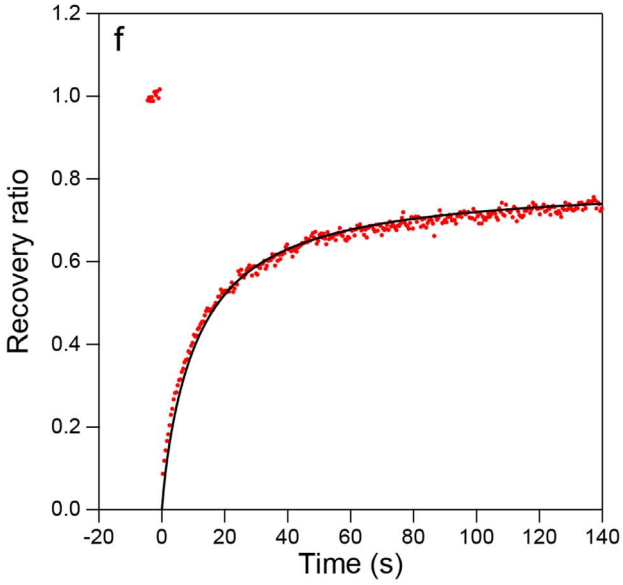

Fig. 4. Fluorescence image in the FRAP process of cationic s-BLMs after adding an anionic vesicle containing 0.5% Rhod-DPPE. (a) Before bleaching, (b) while bleaching ($t = 0$ s), (c) $t = 10$ s, (d) $t = 20$ s, (e) $t = 140$ s. Scale bar: 10 μm. (f) The fluorescence recovery curve of the cationic s-BLMs after vesicle fusion. Dots show results obtained experimentally with the FRAP measurement, and the solid line represents the fitting curve obtained using Eq. (2).

vesicles. We set the parameters of the confocal microscope used to acquire the FRAP images as follows; a sampling speed of 0.429 s/frame (2.0 μs/pixel; image size, 256 × 256 pixels), a bleaching time of 0.858 s, and a bleaching radius of 6.2 μm (50 pixels). The Rhod-DPPE in cationic s-BLMs was bleached so that it became dark with a laser beam (Fig. 4(b)). The lipid molecules diffused in the cationic s-BLMs, thus the fluorescence intensity in the bleached area gradually recovered (Fig. 4(c)–(e)). Fig. 4(f) shows the fluorescence recovery curve obtained by FRAP measurement of the Rhod-DPPE intensity (Fig. 4(a)–(e)). The recovery ratio, which was defined as $f(t) = \frac{\{F(t) - F_0\}}{\{F_- - F_0\}}$, was calculated and fitted with the experimental data. Here, $F(t)$, F_0, and F_- are the total fluorescence intensities in the bleached area at time t, at just after bleaching, and before bleaching, respectively. FRAP analysis has already been established, and in many cases the recovery curve can be described with a simple closed form [24,25]. In this work, however, the diameter of the bleaching area was limited by the size of the patch of the s-BLMs, which were formed by rupturing GUVs. For a small bleaching area, the divergence of the laser beam used for bleaching and the diffusion of the fluorescent dyes during the bleaching process are not negligible. The simple method underestimates the diffusion coefficient. Therefore, we adopted a numerical calculation for the diffusion equation to obtain the theoretical fluorescence recovery curves. In the calculation of the fitted recovery curve, which assumes isotropic diffusion and circular bleaching, the concentration $C(r,t)$ of unbleached fluorophores is represented by the following diffusion equation.

$$\frac{\partial C(r,t)}{\partial t} = D\left\{\frac{1}{r}\frac{\partial C(r,t)}{\partial r} + \frac{\partial^2 C(r,t)}{\partial r^2}\right\} \quad (1)$$

Here, r is the distance from the center of the bleached circle, t is the elapsed time after bleaching is complete, and D is the diffusion coefficient. Bleaching was assumed to have been accomplished by undertaking a uniform scan in the area $r < r_0$ ($r_0 = 6.2$ μm in this experimental condition) with a laser beam that had a Gaussian intensity profile whose standard deviation $\sigma = 1$ μm. The concentrations during and after bleaching were calculated numerically by

$$C_{i,j} = C_{i,j-1} + D\left\{\frac{1}{\Delta r \cdot i}\frac{(C_{i+1,j-1} - C_{i-1,j-1})}{2\Delta r} + \frac{(C_{i+1,j-1} - 2C_{i,j-1} + C_{i-1,j-1})}{\Delta r^2}\right\}\cdot\Delta t \quad (2)$$

with sufficiently small values of $\Delta r = 0.01$ μm and $\Delta t = 0.01$ ms. The position r and the elapsed time t are represented by $r = \Delta r \cdot i$ and $t = \Delta t \cdot j - T_{bleach}$, respectively. Here, T_{bleach} is the bleaching period. During bleaching ($-T_{bleach} \le t < 0$), in addition to the lateral diffusion described by Eq. (2), we also calculated the reduction in $C_{i,j}$ caused by laser irradiation. By fitting the theoretical curve with experimental data, we estimated the diffusion coefficient D and mobile fraction A of Rhod-DPPE in the cationic s-BLMs after fusion of the anionic LUVs to be $D = 1.26 \pm 0.12$ μm^2/s and $A = 0.83 \pm 0.04$ (n = 10), respectively. Here, mobile fraction A is defined as the recovery rate $f(\infty)$ after sufficient time has elapsed. It means that 83% of the Rhod-DPPE could diffuse laterally in the s-BLMs. In the vesicle fusion process, it is well known that there are intermediate stages such as adsorption and hemi-fusion before complete fusion [13]. Hemi-fusion structures represent connections between the outer leaflets of the LUVs and the upper leaflets of the s-BMLs, while the inner leaflets remain distinct. The inner leaflets of the LUVs and the lower leaflets of the s-BMLs combine by forming fusion pores, and the fusion is completed. We assumed that the fusion between the vesicles and the s-BMLs is a similar fusion process to that described in reference [13]. Different fusion processes should be considered at the edge of the s-BML patches. However, it cannot be fully understood from this study. It constitutes a future task. Because some of the LUVs had not completed their fusion process, there was some Rhod-DPPE that could not freely diffuse in the s-BLMs. However, the high value of mobile fraction A indicates that almost all the LUVs attached to the s-BLM were completely fused. As mentioned in Section 3.2, the area increase $\Delta S/S$ agrees with the amount of fusion R. It means that fused LUVs widen the area of the patch. This is consistent with a high mobile fraction. The estimated diffusion coefficient shows a sufficiently high fluidity, and it is also consistent with the fusion process being almost complete. This diffusion coefficient is somewhat larger than that measured for an s-BLM before vesicle fusion. The initial diffusion coefficient (Di) for a cationic s-BLM, which was labeled with Rhod-DPPE instead of NBD-DOPE, was $Di = 0.77 \pm 0.09$ μm^2/s (n = 11) (figure not shown). Vesicle fusion with anionic LUVs neutralized the positive charge in cationic s-BLM and reduced the electrostatic attraction with the substrate. This may be the reason for the changing diffusion coefficient, but the details will be discussed elsewhere. The sufficiently high diffusion coefficient of the s-BLM after vesicle fusion confirmed that we had realized a continuous and fluidic bilayer, which is one of the key requirements for a platform if membrane proteins are to function.

In this study, we have shown that the combination of cationic s-BLMs and anionic LUVs is effective for vesicle fusion control. This control method is also expected to introduce membrane proteins into the s-BLMs. The biological cell membranes contain anionic lipids such as DOPS. Therefore, the membrane fraction containing membrane proteins prepared from the biological cell has some negative charges. It is also common to mix anionic lipids when we prepare the proteoliposomes by reconstitution techniques using purified membrane proteins. Therefore, we will be able to control the fusion into the s-BLMs of membrane fractions or proteoliposomes with some negative charges.

4. Conclusions

In conclusion, we demonstrated the control of vesicle fusion by employing an electrostatic interaction between cationic s-BLMs and anionic LUVs. The anionic vesicle fused selectively with the cationic s-BLMs. The vesicle fusion was enhanced as the cationic lipid concentration increased. These results suggest that we can control the amount of LUV fusion by changing the cationic lipid concentration. We also confirmed that there are not many intermediate state vesicles in the fusion process, and the fluidity of the s-BLMs after vesicle fusion is sufficiently high for device applications. Furthermore, this electrostatic method for controlling vesicle fusion could also be applied to the introduction of membrane proteins into s-BLMs, because membrane proteins extracted from biological cells are generally included in liposomes containing DOPS and DOPC.

Acknowledgements

We thank Wataru Kurata for his experimental support throughout this research.

Appendix A. Transparency document

Supplementary data associated with this article can be found in the online version at http://dx.doi.org/10.1016/j.bbrep.2017.06.003.

References

[1] E. Sackmann, Science 271 (1996) 46.
[2] E.T. Castellana, P.S. Cremer, Surf. Sci. Rep. 61 (2006) 429.
[3] R. Tero, Materials 5 (2012) 2658.
[4] L. Stamatatos, R. Leventis, M.J. Zuckermann, K.R. Silvius, Biochem 27 (1988) 3917.
[5] K. Simons, The Biology of Lipids: Trafficking, Regulation, and Function, Cold Spring Harbor Laboratory Press, New York, 2011.
[6] C. Miller, Ion Channel Reconstitution, Plenum Press, New York, 1986.
[7] H. Bayley, P.C. Cremer, Nature 413 (2001) 226.
[8] A. Kleefen, D. Pedone, C. Grunwald, R. Wei, M. Firnkes, G. Abstreiter, U. Rant, R. Tampe, Nano Lett. 10 (2010) 5080.
[9] K. Sumitomo, A. McAlister, Y. Tamba, Y. Kashimura, A. Tanaka, Y. Shinozaki, K. Torimitsu, Biosens. Bioelectron. 31 (2012) 445.
[10] A. Hirano-Iwata, Y. Ishinari, H. Yamamoto, M. Niwano, Chem. Asian J. 10 (2016) 1266.

[11] Y. Shinozaki, K. Sumitomo, A. Tanaka, N. Kasai, K. Torimitsu, Appl. Phys. Exp. 4 (2011) 107001.
[12] L. Tiefenauer, S. Demarche, Materials 5 (2012) 2205.
[13] L.V. Chernomordik, M.M. Kozlov, Nat. Struct. Mol. Biol. 15 (2008) 675.
[14] D. Tareste, J. Shen, T.J. Melia, J.E. Rothman, Proc. Natl. Acad. Sci. USA 105 (2008) 2380.
[15] L.L.G. Schwenen, R. Hubrich, D. Milovanovic, B. Geil, J. Yang, A. Kros, R. Jahn, C. Steinem, Sci. Rep. 5 (2015) 12006.
[16] G. Stengel, R. Zahn, F. Höök, J. Am. Chem. Soc. 129 (2007) 9584.
[17] A. Hirano-Iwata, Y. Ishinari, M. Yoshida, D. Tadaki, R. Miyata, K. Ishibashi, H. Yamamoto, Y. Kimura, M. Niwano, Biophys. J. 110 (2016) 2207.
[18] R.W. Malone, P.L. Felgner, I.M. Verma, Proc. Natl. Acad. Sci. USA 86 (1989) 6077.
[19] M.S. Yeganeh, S.M. Dougal, H.S. Pink, Phys. Rev. Lett. 83 (1999) 1179.
[20] D.S. Dimitrov, M.I. Angelova, Bioelectrochem. Bioenergy 19 (2002) 1235.
[21] M. Traïkia, D.E. Warschawski, M. Recouvreur, J. Cartaud, P.F. Devaux *Eur. Biophys. J.*, **29** (200) 184.
[22] J.N. Israelachvili, Intermolecular and Surface Forces, Academic Press, London, 1992.
[23] R. Richter, A. Mukhopadhyay, A. Brisson, Biophys. J. 85 (2003) 3035.
[24] D. Axelrod, D.E. Koppel, J. Schlessinger, E. Elson, W.W. Webb, Biophys. J. 16 (1976) 1055.
[25] D.M. Soumpass, Biophys. J. 41 (1983) 95.